



TEXAS
The University of Texas at Austin

COVID-19 in Austin, Texas: Epidemiological Assessment of Construction Work

Remy Pasco, Dr. Zhanwei Du, Xutong Wang, Michaela Petty, Dr. Spencer J. Fox,
Dr. Lauren Ancel Meyers

CORRESPONDING AUTHOR

Lauren Ancel Meyers
The University of Texas at Austin
laurenmeyers@gmail.com

COVID-19 in Austin, Texas: Epidemiological Assessment of Construction Work

Remy Pasco, Dr. Zhanwei Du, Xutong Wang, Michaela Petty, Dr. Spencer J. Fox, Dr. Lauren Ancel Meyers

Corresponding author:
Lauren Ancel Meyers
The University of Texas at Austin
laurenmeyers@gmail.com

Overview

There are an estimated 50,000 construction workers in the Austin metropolitan area representing over 4% of the labor force [1], not accounting for undocumented workers.

The Austin *Stay Home - Work Safe* order that was issued on March 24, 2020 limits construction work [2]. Since many construction workers live off of weekly income, those restricted from non-essential worksites may seek work at essential worksites. This may not only undermine efforts to reduce person-to-person contact, but exacerbate the individual and city-wide risk by increasing the number of workers in close contact at single construction sites.

In response to a request from the city of Austin, we projected the epidemiological impacts of allowing some or all construction workers to resume work. To do so, we modified the Austin-Round Rock module of our *US COVID-19 Pandemic Model* to explicitly include a population subgroup representing construction workers. We considered several different scenarios in which we varied the contact intensity among construction workers at worksites and the proportion of workers allowed to work.

As a base case scenario, we assumed that construction workers would maintain typical workforce contact rates, estimated for 18-49 year olds. As a highest risk scenario, we assumed that the workers would have double the typical contact rate. This might be the case if construction workers have higher than average contact rates in general, or if contacts are elevated by workers migrating from a large number of non-essential to a smaller number of essential worksites. As a lower risk scenario, we reduce the

workplace contacts by 50%. This might occur if precautionary measures are implemented as has been discussed by city officials, including thorough cleaning of equipment between uses, increased use of protective equipment such as gloves and masks, limits on the number of workers on a given site, and ramped up health surveillance on worksites including daily temperature readings, rapid COVID-19 testing with symptoms, contact tracing and isolation of cases and known contacts of workers who test positive for COVID-19.

The projections suggest that the incremental community risk of allowing construction work depends on three key factors:

- *Efficacy of Stay Home-Work Safe*: Perhaps surprisingly, construction work is most detrimental under scenarios where the social distancing order is *highly* effective. If the order is highly effective, then the additional COVID-19 transmission within the construction worker community can undermine the strong mitigation achieved. If the order is only moderately effective, the additional transmission caused by construction work may be marginal.
- *Size of construction workforce*: Generally, the larger the population of active workers, the faster COVID-19 will spread. However, this effect is only strong under the scenario of highly effective social distancing.
- *Risk of transmission at construction work sites*: Generally, the greater the risk of transmission at construction job sites, the faster COVID-19 will spread. As with the size of the construction workforce, this is more apparent under the scenario of highly effective social distancing.

Our projections also suggest that the risk of severe COVID-19 within the construction workforce will be higher than that in the non-construction working 18-49 year old populations. Large numbers of workers and high job site risk exacerbate this disparity. Under a scenario of effective social distancing and a large construction workforce, the hospitalization risk is expected to be two to three times higher for construction workers than non-construction workers.

Scenarios

We updated the Austin-Round Rock module of our *US COVID-19 Pandemic Model* to simulate COVID-19 epidemics under various scenarios that allow partial or all construction work to proceed during the *Stay Home-Work Safe* order. The simulations ran from April 1 through mid-August, 2020. They assume the following initial conditions and key parameters:

- Starting condition: April 1, 2020 with 346 infected adults
- Epidemic doubling time: 4 days [3]
- Reproduction number: 2.2 [4]
- Average incubation period: 6.9 days [5]
- Proportion of cases asymptomatic: 17.9% [6]

All other model parameters, including age-specific hospitalization and fatality rates are provided in the Appendix.

All of the scenarios we analyzed assume that Austin's *Stay Home - Work Safe* order has effectively reduced non-household contacts by either 75% or 90%. We estimate the impact of the Austin population of 50,000 construction workers continuing to work at the following levels:

- 0%, 25%, 50%, 75% or 100% continue to work at construction sites
- Contact rates between active construction workers are either equal to baseline contact rates for 18-49 year old workers, half of that baseline (50%) and twice that baseline (200%)

Projections

Highly effective Stay Home-Work Safe (90%)

Overall increase in hospitalization risk: Assuming that the *Stay Home-Work Safe* order is highly effective, allowing all construction work to proceed would be expected to triple the number of COVID-19 hospitalizations in the Austin-Round Rock Area, under the scenario that construction job sites have double the transmission risk of a typical workplace (Figure 1). Measures to reduce risk of transmission at job sites could mitigate this risk.

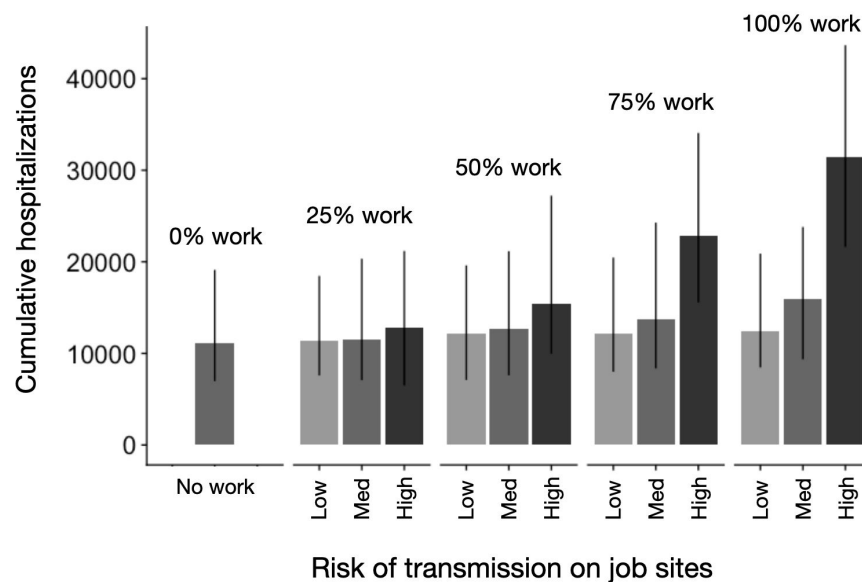


Figure 1. Projected cumulative hospitalizations in the Austin-Round Rock MSA through mid-August under different workforce scenarios. Bars and error bars indicate minimum, median and maximum across 100 stochastic simulations. Shading indicates level of risk of transmission at construction work sites: light gray is half the risk of a typical workplace; medium gray is typical workplace risk; dark gray is twice the risk of a typical workplace.

Increase in risk among construction workers: Assuming that the Stay Home-Work Safe order is highly effective, allowing all construction work to proceed would disproportionately increase risk among construction workers. Allowing all construction work to proceed would lead to an estimated eight-fold increase in the number of construction workers that are hospitalized for COVID-19 by mid-August, under the scenario that construction job sites have double the transmission risk of a typical workplace (Figure 2). Measures to reduce risk of transmission at job sites could mitigate but not eliminate this risk.



Figure 2. Projected cumulative hospitalizations in the Austin-Round Rock MSA construction workforce through mid-August under different workforce scenarios. Bars and points indicate minimum, median and maximum across 100 stochastic simulations. Shading indicates level of risk of transmission at construction work sites: light gray is half the risk of a typical workplace; medium gray is typical workplace risk; dark gray is twice the risk of a typical workplace.

Projected COVID-19 hospitalizations under various construction workforce

scenarios: Assuming that *Stay Home-Work Safe* has reduced non-household contacts by 90%, we estimate that construction work will slightly accelerate pandemic spread. If all workers are permitted to continue work, we estimate that the cumulative hospitalizations in the Austin-Round Rock MSA as a whole through mid-August will increase by 9.2%, 39.5% or 175.5% depending on whether worksite conditions either reduce COVID-19 transmission by 50%, do not impact onsite transmission, or increase transmission two-fold, respectively (Figure 3). The most extreme scenario (100% workforce with two-fold elevated worksite) would be expected to elevate COVID-19 hospitalizations beyond local healthcare capacity by early July. If precautions are taken to reduce contacts on worksites, such a crisis could be averted.

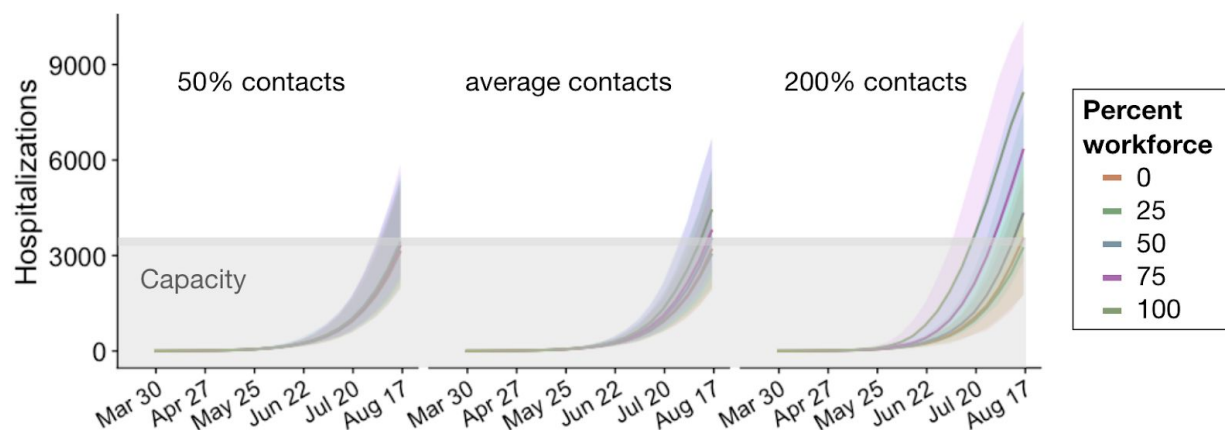


Figure 3. Projected impact of construction work on COVID-19 hospitalizations in the Austin-Round Rock MSA through mid-August, assuming that Austin's *Stay Home-Work Safe* order has reduced non-household contacts by 90%. From left to right, the graphs consider three scenarios for onsite transmission: 50% reduced transmission through precautionary measures; average workplace transmission rates for adults 18-49y; two-fold increased transmission relative to typical workplace because of nature of construction work and/or elevated concentration of construction workers at *essential* worksites. Colors indicate the fraction of the construction workforce allowed to work. Shaded area indicates the estimated hospital capacity of 80% of 4299 hospital beds in the Austin-Round Rock MSA.

Moderately effective Stay Home-Work Safe (75%)

Overall increase in hospitalization risk: Assuming that the *Stay Home-Work Safe* order is moderately effective, allowing all construction work to proceed would be expected to increase the number of COVID-19 hospitalizations in the Austin-Round Rock Area by at least 10,000 by mid-August, under the scenario that construction job sites have double the transmission risk of a typical workplace (Figure 4). Measures to reduce risk of transmission at job sites could mitigate this risk.



Figure 4. Projected cumulative hospitalizations in the Austin-Round Rock MSA through mid-August under different workforce scenarios.

Bars and points indicate minimum, median and maximum across 100 stochastic simulations. Shading indicates level of risk of transmission at construction work sites: light gray is half the risk of a typical workplace; medium gray is typical workplace risk; dark gray is twice the risk of a typical workplace.

Increase in risk among construction workers: Assuming that the Stay Home-Work Safe order is effective, allowing all construction work to proceed would disproportionately increase risk among construction workers. Allowing all construction work to proceed would be expected to double the number of construction workers that are hospitalized for COVID-19 by mid-August, under the scenario that construction job sites have double the transmission risk of a typical workplace (Figure 5). Measures to reduce risk of transmission at job sites could mitigate but not eliminate this risk.

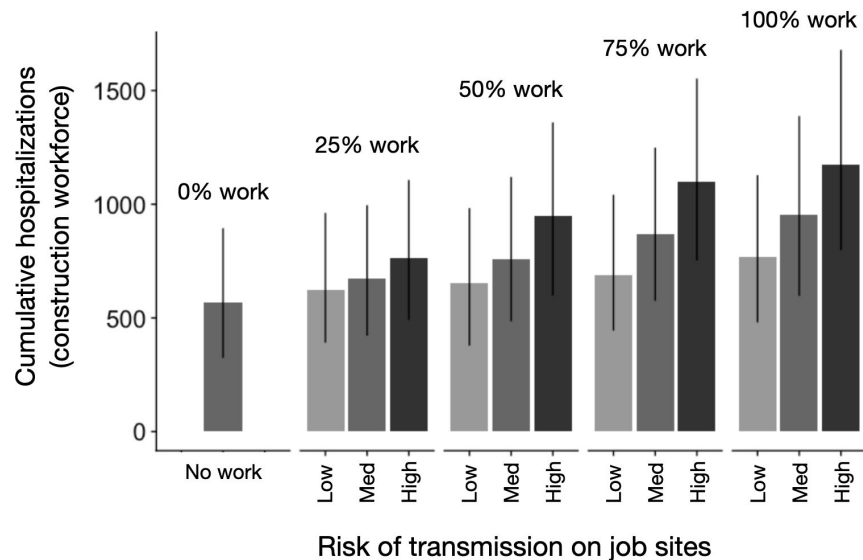


Figure 5. Projected cumulative hospitalizations in the Austin-Round Rock MSA construction workforce through mid-August under different workforce scenarios. Bars and points indicate minimum, median and maximum across 100 stochastic simulations. Shading indicates level of risk of transmission at construction work sites: light gray is half the risk of a typical workplace; medium gray is typical workplace risk; dark gray is twice the risk of a typical workplace.

Projected COVID-19 hospitalizations under various construction workforce scenarios:

Assuming that *Stay Home-Work Safe* has reduced non-household contacts by 75%, we estimate that construction work will slightly accelerate pandemic spread. If all workers are permitted to continue work, we estimate that the cumulative hospitalizations in the Austin-Round Rock MSA as a whole through mid-August will increase by 5.9%, 10.4% or 30.3% depending on whether worksite conditions either reduce COVID-19 transmission by 50%, do not impact onsite transmission, or increase transmission two-fold, respectively (Figure 6). If construction work is completely banned, we would expect COVID-19 hospitalizations to exceed local capacity around July 26, 2020. The most extreme scenario (100% workforce with two-fold elevated worksite) would accelerate this crisis in healthcare by an estimated two weeks.

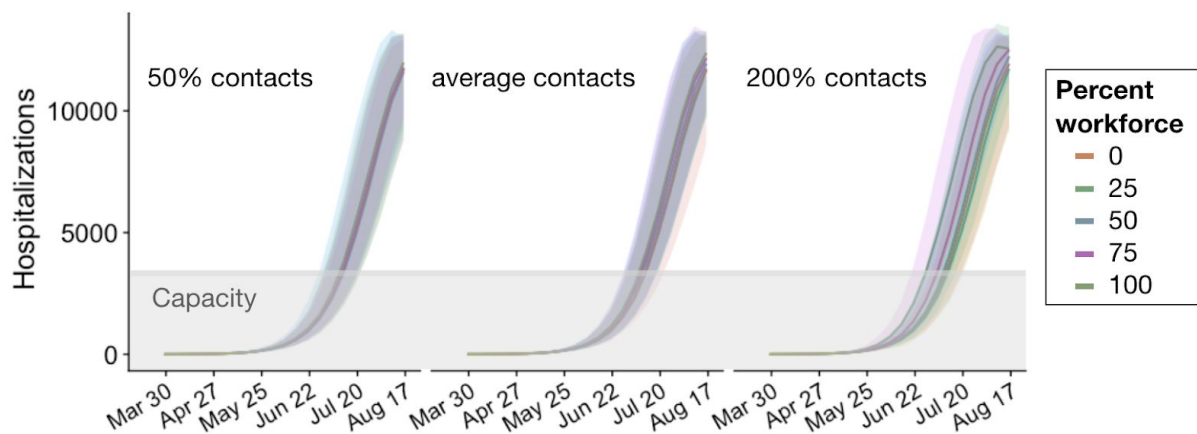


Figure 6. Projected impact of construction work on COVID-19 hospitalizations in the Austin-Round Rock MSA through mid-August, assuming that Austin’s *Stay Home-Work Safe* order has reduced non-household contacts by 75%. From left to right, the graphs consider three scenarios for onsite transmission: 50% reduced transmission through precautionary measures; average workplace transmission rates for adults 18-49y; two-fold increased transmission relative to typical workplace because of nature of construction work and/or elevated concentration of construction workers at *essential* worksites. Colors indicate the fraction of the construction workforce allowed to work. Shaded area indicates the estimated hospital capacity of 80% of 4299 hospital beds in the Austin-Round Rock MSA.

Appendix

COVID-19 Epidemic Model Structure and Parameters

The model structure is diagrammed in Figure A1 and described in the equations below.

For each age and risk group, we build a separate set of compartments to model the transitions between the states: susceptible (S), exposed (E), symptomatic infectious (I^Y), asymptomatic infectious (I^A), symptomatic infectious that are hospitalized (I^H), recovered (R), and deceased (D). The symbols S, E, I^Y , I^A , I^H , R, and D denote the number of people in that state in the given age/risk group and the total size of the age/risk group is $N = S + E + I^Y + I^A + I^H + R + D$.

The model for individuals in age group a and risk group r is given by:

$$\begin{aligned}\frac{dS_{a,r}}{dt} &= - \sum_{i \in A} \sum_{j \in K} (I_{i,j}^Y \omega^Y + I_{i,j}^A \omega^A + E_{i,j} \omega^E) \beta \phi_{a,i} / N_i \\ \frac{dE_{a,r}}{dt} &= \sum_{i \in A} \sum_{j \in K} (I_{i,j}^Y \omega^Y + I_{i,j}^A \omega^A + E_{i,j} \omega^E) \beta \phi_{a,i} / N_i - \sigma E_{a,r} \\ \frac{dI_{a,r}^A}{dt} &= (1 - \tau) \sigma E_{a,r} - \gamma^A I_{a,r}^A \\ \frac{dI_{a,r}^Y}{dt} &= \tau \sigma E_{a,r} - (1 - \pi) \gamma^Y I_{a,r}^Y - \pi \eta I_{a,r}^Y \\ \frac{dI_{a,r}^H}{dt} &= \pi \eta I_{a,r}^Y - (1 - \nu) \gamma^H I_{a,r}^H - \nu \mu I_{a,r}^H \\ \frac{dR_{a,r}}{dt} &= \gamma^A I_{a,r}^A + (1 - \pi) \gamma^Y I_{a,r}^Y + (1 - \nu) \gamma^H I_{a,r}^H \\ \frac{dD_{a,r}}{dt} &= \nu \mu I_{a,r}^H\end{aligned}$$

where A and K are all possible age and risk groups, I^A , I^Y , I^H are relative infectiousness of the I^A , I^Y , I^H compartments, respectively, β is transmission rate, $\phi_{a,i}$ is the mixing rate between age group a , $i \in A$, ω^A , ω^Y , ω^H are the recovery rates for the I^A , I^Y , I^H compartments, respectively, σ is the exposed rate, τ is the symptomatic ratio, π is the proportion of symptomatic individuals requiring hospitalization, η is rate at which hospitalized cases enter the hospital following symptom onset, ν is mortality rate for hospitalized cases, and μ is rate at which terminal patients die.

We model stochastic transitions between compartments using the τ -leap method[7,8] with key parameters given in Table S1. Assuming that the events at each time-step are independent and do not impact the underlying transition rates, the numbers of each type of event should follow Poisson distributions with means equal to the rate parameters. We thus simulate the model according to the following equations:

$$\begin{aligned}S_{a,r}(t+1) - S_{a,r}(t) &= -P_1 \\ E_{a,r}(t+1) - E_{a,r}(t) &= P_1 - P_2 \\ I_{a,r}^A(t+1) - I_{a,r}^A(t) &= (1 - \tau)P_2 - P_3 \\ I_{a,r}^Y(t+1) - I_{a,r}^Y(t) &= \tau P_2 - P_4 - P_5 \\ I_{a,r}^H(t+1) - I_{a,r}^H(t) &= P_5 - P_6 - P_7\end{aligned}$$

$$R_{a,r}(t+1) - R_{a,r}(t) = P_3 + P_4 + P_6$$

$$D_{a,r}(t+1) - D_{a,r}(t) = P_7,$$

with

$$P_1 \sim \text{Pois}(S_{a,r}(t)F_{a,r}(t))$$

$$P_2 \sim \text{Pois}(\sigma E_{a,r}(t))$$

$$P_3 \sim \text{Pois}(\gamma^A I_{a,r}^A(t))$$

$$P_4 \sim \text{Pois}((1 - \pi)\gamma^Y I_{a,r}^Y(t))$$

$$P_5 \sim \text{Pois}(\pi\eta I_{a,r}^Y(t))$$

$$P_6 \sim \text{Pois}((1 - \nu)\gamma^H I_a^H)$$

$$P_7 \sim \text{Pois}(\nu\mu I_{a,r}^H(t))$$

and where $F_{a,r}$ denotes the force of infection for individuals in age group a and risk group r and is given by:

$$F_{a,r}(t) = \sum_{i \in A} \sum_{j \in K} (I_{i,r}^Y(t)\omega^Y + I_{i,r}^A(t)\omega^A + E_{i,j}(t)\omega^E)\beta_{a,i}\phi_{a,i}/N_i$$

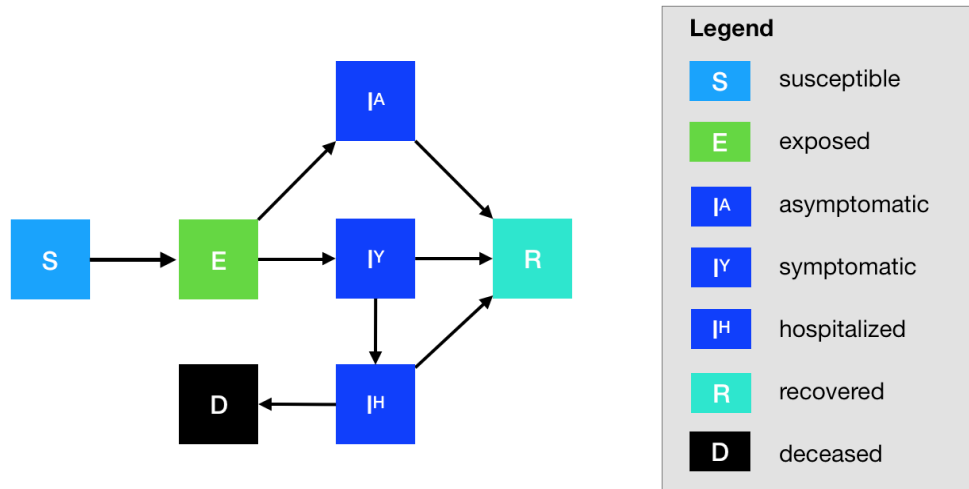


Figure A1. Compartmental model of COVID-19 transmission in a US city. Each subgroup (defined by age, risk and worker-type) is modeled with a separate set of compartments. Upon infection, susceptible individuals (S) progress to exposed (E) and then to either symptomatic infectious (I^Y) or asymptomatic infectious (I^A). All asymptomatic cases eventually progress to a recovered class where they remain protected from future infection (R); symptomatic cases are either hospitalized (I^H) or recover. Mortality (D) varies by age group and risk group and is assumed to be preceded by hospitalization.

Table A1. Initial conditions, school closures and social distancing policies

Variable	Settings
Initial day of simulation	4/1/2020
Initial infection number in locations	346 symptomatic cases in 18-49y age group
Trigger to close school	4/1/2020
Closure Duration	Until start of 2020-2021 school year (8/17/20)
a: social distancing reduction of other non-household contacts	Two scenarios: [0.75, 0.9]
b: proportion construction workers who continue to work	Five scenarios: [0, 0.25, 0.5, 0.75, 1]
c: contact rates at work between active construction workers are equal to baseline contact rates for 18-49 year old works multiplied by a scaling factor	Three scenarios for scaling factor: [0.5, 1, 2]
work_CW: contact matrix of construction workers	Work matrices provided in Tables S5.1-S5.4 work_CW = work - work(1:5, 1:5)
Age-specific and day-specific contact rates	Home, work, other and school matrices provided in Tables S5.1-S5.4 Weekday = home + (1-a)*(work + other) + b*c*work_CW Weekend = home + (1-a)*(other) Weekday holiday = home + (1-a)*(other)

Table A2. Model parameters^a

Parameters	Best guess values	Source
R_0	2.2	Li et al. [3]
δ : doubling time	4 days	Kraemer et al.[4]
β : transmission rate	0.0260	Fitted ^a to obtain specified R_0 given δ
γ^A : recovery rate on asymptomatic compartment	Equal to γ^Y	
γ^Y : recovery rate on symptomatic non-treated compartment	$\frac{1}{\gamma^Y} \sim \text{Triangular}(21.2, 22.6, 24.4)$	Verity et al. [9]
τ : symptomatic proportion (%)	82.1	Mizumoto et al.[6]
σ : exposed rate	$\frac{1}{\sigma} \sim \text{Triangular}(5.6, 7, 8.2)$	Lauer et al.[5]
P : proportion of pre-symptomatic (%)	12.6	Du et al.[10]
ω^E : relative infectiousness of infectious individuals in compartment E	$\omega^E = \frac{(\frac{Y_{HR}}{\eta} + \frac{1-Y_{HR}}{\gamma^Y})\omega^Y \sigma P}{1-P}$	

ω^A : relative infectiousness of infectious individuals in compartment I ^A	0.4653	Set to mean of ω^E
<i>IFR</i> : infected fatality ratio, age specific (%)	Overall: [0.0016, 0.0049, 0.0840, 1.0000, 3.3710] Low risk: [0.0009, 0.0022, 0.0339, 0.2520, 0.6440] High risk: [0.0092, 0.0218, 0.3388, 2.5197, 6.4402]	Age adjusted from Verity et al.[9]
<i>YFR</i> : symptomatic fatality ratio, age specific (%)	Overall: [0.0019, 0.0060, 0.1027, 1.2182, 4.1066] Low risk: [0.0011165, 0.0027, 0.0412, 0.3069, 0.7844] High risk: [0.0112, 0.0265, 0.4126, 3.0690, 7.8443]	$YFR = \frac{IFR}{1-\tau}$
<i>h</i> : high-risk proportion, age specific (%)	[8.2825, 14.1121, 16.5298, 32.9912, 47.0568]	Estimated using 2015-2016 Behavioral Risk Factor Surveillance System (BRFSS) data with multilevel regression and poststratification using CDC's list of conditions that may increase the risk of serious complications from influenza[11–13]
<i>rr</i> : relative risk for high risk people compared to low risk in their age group	10	Assumption
School calendars	Austin Independent School District calendar (2019-2020, 2020-2021)[14]	

^aValues given as five-element vectors are age-stratified with values corresponding to 0-4, 5-17, 18-49, 50-64, 65+ year age groups, respectively.

Table A3 Hospitalization parameters

Parameters	Value	Source
γ^H : recovery rate in hospitalized compartment	1/14	14 day-average from admission to discharge (UT Austin Dell Med)
YHR : symptomatic case hospitalization rate (%)	Overall: [0.0487, 0.0487, 3.2876, 11.3373, 17.7330] Low risk: [0.0279, 0.0215, 1.3215, 2.8563, 3.3873] High risk: [0.2791, 0.2146, 13.2154, 28.5634, 33.8733]	Age adjusted from Verity et al. [9]
π : rate of symptomatic individuals go to hospital, age-specific	$\pi = \frac{\gamma^Y * YHR}{\eta + (\gamma^Y - \eta)YHR}$	
η : rate from symptom onset to hospitalized	0.1695	5.9 day average from symptom onset to hospital admission Tindale et al.[15]
μ : rate from hospitalized to death	1/14	14 day-average from admission to death (UT Austin Dell Med)
HFR : hospitalized fatality ratio, age specific (%)	[4, 12.365, 3.122, 10.745, 23.158]	$HFR = \frac{IFR}{YHR(1-\tau)}$
ν : death rate on hospitalized individuals, age specific	[0.0390, 0.1208, 0.0304, 0.1049, 0.2269]	$\nu = \frac{\gamma^H HFR}{\mu + (\gamma^H - \mu)HFR}$
Healthcare capacity	Hospital beds: 4299	Regional hospitals

^a The parameter β is fitted through constrained trust-region optimization in SciPy/Python.[16] Given a value of β , a deterministic simulation is run based on central values for each parameter, from which we can compute the implied $\bar{R}_0(\beta)$. We (1) track the daily number of new cases I_t (both symptomatic and asymptomatic) during the exponential growth portion of the epidemic, (2) compute the log of the number of new cases: $y_t = \log(I_t)$ and (3) use least squares to fit a line to this curve: $\log(I_t) = y_0 + g \cdot t$. We then estimate the reproduction number $\bar{R}_0(\beta)$ of the simulation for that specific value of β as $\bar{R}_0(\beta) = \Gamma \cdot g + 1$ where Γ is the generation time given by $\Gamma = \frac{\delta(R_0-1)}{\log(2)}$. The optimizing function runs until the resulting value of $\bar{R}_0(\beta)$ does not get closer to the target value.

Model modification to incorporate construction workforce

We assume there are currently 50,000 construction workers in the Austin-Round Rock MSA, all in the 18-49 year-old age group. The proportion of construction workers at high-risk of complications from COVID-19 is the same as the overall 18-49y age group in the Austin-Round Rock MSA.

We extended our *US COVID-19 Pandemic Model* to include a separate population subgroup representing construction workers. We moved 50,000 individuals from the *regular* 18-49y low risk and high risk compartments into the corresponding *construction* compartments. We also extended the contact matrices [17] governing transmission between age groups to allow us to manipulate the number of construction workers and intensity of their contacts separately from the rest of the workforce. Initially, we set their contact rates equal to those of the entire 18-49y population, except that we assume that all work contacts take place within the subgroup of construction workers. Social distancing measures reduce *work* and *other* contacts for non-construction workers and *other* contacts for construction workers (by either 75% or 90%). Tables A4.1-A4.4 give the original contact matrices and Tables A5.1-A5.4 give the updated contact matrices assuming 50,000 construction workers.

Let $C(X)_{i,j}$ denote the average daily number of contacts that a person in group i has with people in group j at location X . Let w denote the proportion of construction workers in the 18-49y group.

For each age group i the new work (W) contact matrix between groups other than construction workers is unchanged:

$$\begin{aligned} C'(W)_{i,j} &= C(W)_{i,j} \text{ for } j \neq \text{Construction} \\ C'(W)_{i,\text{Construction}} &= 0 \end{aligned}$$

Construction workers only have contacts among themselves at work so:

$$\begin{aligned} C'(W)_{\text{Construction},\text{Construction}} &= \sum_j C(W)_{18-49,j} \\ C'(W)_{\text{Construction},j} &= 0 \text{ for other groups } j \end{aligned}$$

For contacts at home, school and other locations we assume that construction workers have the same contact patterns as any other 18-49 years old individual. Then at those locations (X) the contacts a person has with individuals in the 18-49y group is simply split between the existing 18-49y column and the new construction column:

$$\begin{aligned} C'(X)_{i,18-49} &= C(X)_{i,18-49} * (1 - w) \\ C'(X)_{i,\text{Construction}} &= C(X)_{i,18-49} * w \\ C'(X)_{\text{Construction},j} &= C(X)_{18-49,j} \end{aligned}$$

Original 5-age groups contact matrices

Table A4.1 Home contact matrix. Daily number contacts by age group at home.

	0-4y	5-17y	18-49y	50-64y	65y+
0-4y	0.5	0.9	2.0	0.1	0.0
5-17y	0.2	1.7	1.9	0.2	0.0
18-49y	0.2	0.9	1.7	0.2	0.0
50-64y	0.2	0.7	1.2	1.0	0.1
65y+	0.1	0.7	1.0	0.3	0.6

Table A4.2 School contact matrix. Daily number contacts by age group at school.

	0-4y	5-17y	18-49y	50-64y	65y+
0-4y	1.0	0.5	0.4	0.1	0.0
5-17y	0.2	3.7	0.9	0.1	0.0
18-49y	0.0	0.7	0.8	0.0	0.0
50-64y	0.1	0.8	0.5	0.1	0.0
65y+	0.0	0.0	0.1	0.0	0.0

Table A4.3 Work contact matrix. Daily number contacts by age group at work.

	0-4y	5-17y	18-49y	50-64y	65y+
0-4y	0.0	0.0	0.0	0.0	0.0
5-17y	0.0	0.1	0.4	0.0	0.0
18-49y	0.0	0.2	4.5	0.8	0.0
50-64y	0.0	0.1	2.8	0.9	0.0
65y+	0.0	0.0	0.1	0.0	0.0

Table A4.4 Others contact matrix. Daily number contacts by age group at other locations.

	0-4y	5-17y	18-49y	50-64y	65y+
0-4y	0.7	0.7	1.8	0.6	0.3
5-17y	0.2	2.6	2.1	0.4	0.2
18-49y	0.1	0.7	3.3	0.6	0.2
50-64y	0.1	0.3	2.2	1.1	0.4
65y+	0.0	0.2	1.3	0.8	0.6

Updated contact matrices with separate subgroup for construction workers

Table A5.1 Home contact matrix. Daily number contacts by age group at home assuming 50,000 construction workers in Austin MSA.

	0-4y	5-17y	18-49y	50-64y	65y+	Construction
0-4y	0.5	0.9	1.9	0.1	0.0	0.1
5-17y	0.2	1.7	1.8	0.2	0.0	0.1
18-49y	0.2	0.9	1.6	0.2	0.0	0.1
50-64y	0.2	0.7	1.2	1.0	0.1	0.1
65y+	0.1	0.7	0.9	0.3	0.6	0.0
Construction	0.2	0.9	1.6	0.2	0.0	0.1

Table A5.2 School contact matrix. Daily number contacts by age group at school assuming 50,000 construction workers in Austin MSA.

	0-4y	5-17y	18-49y	50-64y	65y+	Construction
0-4y	1.0	0.5	0.4	0.1	0.0	0.0
5-17y	0.2	3.7	0.9	0.1	0.0	0.0
18-49y	0.0	0.7	0.8	0.0	0.0	0.0
50-64y	0.1	0.8	0.4	0.1	0.0	0.0
65y+	0.0	0.0	0.0	0.0	0.0	0.0
Construction	0.0	0.7	0.8	0.0	0.0	0.0

Table A5.3 Work contact matrix. Daily number contacts by age group at work assuming 50,000 construction workers in Austin MSA.

	0-4y	5-17y	18-49y	50-64y	65y+	Construction
0-4y	0.0	0.0	0.0	0.0	0.0	0.0
5-17y	0.0	0.1	0.4	0.0	0.0	0.0
18-49y	0.0	0.2	4.5	0.8	0.0	0.0
50-64y	0.0	0.1	2.8	0.9	0.0	0.0
65y+	0.0	0.0	0.1	0.0	0.0	0.0
Construction	0.0	0.0	0.0	0.0	0.0	5.5

Table A5.4 Others contact matrix. Daily number contacts by age group at other locations assuming 50,000 construction workers in Austin MSA.

	0-4y	5-17y	18-49y	50-64y	65y+	Construction
0-4y	0.7	0.7	1.7	0.6	0.3	0.1
5-17y	0.2	2.6	2.0	0.4	0.2	0.1
18-49y	0.1	0.7	3.1	0.6	0.2	0.2
50-64y	0.1	0.3	2.1	1.1	0.4	0.1
65y+	0.0	0.2	1.2	0.8	0.6	0.1
Construction	0.1	0.7	3.1	0.6	0.2	0.2

Estimation of age-stratified proportion of population at high-risk for COVID-10 complications

We estimate age-specific proportions of the population at high risk of complications from COVID-19 based on data for Austin, TX and Round-Rock, TX from the CDC's 500 cities project (Figure A2).[18] We assume that high risk conditions for COVID-19 are the same as those specified for influenza by the CDC.[11] The CDC's 500 cities project provides city-specific estimates of prevalence for several of these conditions among adults.[19] The estimates were obtained from the 2015-2016 Behavioral Risk Factor Surveillance System (BRFSS) data using a small-area estimation methodology called multi-level regression and poststratification.[12,13] It links geocoded health surveys to high spatial resolution population demographic and socioeconomic data.[13]

Estimating high-risk proportions for adults. To estimate the proportion of adults at high risk for complications, we use the CDC's 500 cities data, as well as data on the prevalence of HIV/AIDS, obesity and pregnancy among adults (Table A6).

The CDC 500 cities dataset includes the prevalence of each condition on its own, rather than the prevalence of multiple conditions (e.g., dyads or triads). Thus, we use separate co-morbidity estimates to determine overlap. Reference about chronic conditions[20] gives US estimates for the proportion of the adult population with 0, 1 or 2+ chronic conditions, per age group. Using this and the 500 cities data we can estimate the proportion of the population p_{HR} in each age group in each city with at least one chronic condition listed in the CDC 500 cities data (Table A6) putting them at high-risk for flu complications.

HIV: We use the data from table 20a in CDC HIV surveillance report[21] to estimate the population in each risk group living with HIV in the US (last column, 2015 data). Assuming independence between HIV and other chronic conditions, we increase the proportion of the population at high-risk for influenza to account for individuals with HIV but no other underlying conditions.

Morbid obesity: A BMI over 40kg/m² indicates morbid obesity, and is considered high risk for influenza. The 500 Cities Project reports the prevalence of obese people in each city with BMI over 30kg/m² (not necessarily morbid obesity). We use the data from table 1 in Sturm and Hattori[22] to estimate the proportion of people with BMI>30 that actually have BMI>40 (across the US); we then apply this to the 500 Cities obesity data to estimate the proportion of people who are morbidly obese in each city. Table 1 of Morgan et al.[23] suggests that 51.2% of morbidly obese adults have at least one other high risk chronic condition, and update our high-risk population estimates accordingly to account for overlap.

Pregnancy: We separately estimate the number of pregnant women in each age group and each city, following the methodology in CDC reproductive health report.[24] We assume independence between any of the high-risk factors and pregnancy, and further assume that half the population are women.

Estimating high-risk proportions for children. Since the 500 Cities Project only reports data for adults 18 years and older, we take a different approach to estimating the proportion of children at high risk for severe influenza. The two most prevalent risk factors for children are asthma and obesity; we also account for childhood diabetes, HIV and cancer.

From Miller et al.[25], we obtain national estimates of chronic conditions in children. For asthma, we assume that variation among cities will be similar for children and adults. Thus, we use the relative prevalences of asthma in adults to scale our estimates for children in each city. The prevalence of HIV and cancer in children are taken from CDC HIV surveillance report[21] and cancer research report,[26] respectively.

We first estimate the proportion of children having either asthma, diabetes, cancer or HIV (assuming no overlap in these conditions). We estimate city-level morbid obesity in children using the estimated morbid obesity in adults multiplied by a national constant ratio for each age

group estimated from Hales et al.,[27] this ratio represents the prevalence in morbid obesity in children given the one observed in adults. From Morgan et al.,[23] we estimate that 25% of morbidly obese children have another high-risk condition and adjust our final estimates accordingly.

Resulting estimates. We compare our estimates for the Austin-Round Rock Metropolitan Area to published national-level estimates[28] of the proportion of each age group with underlying high risk conditions (Table A6). The biggest difference is observed in older adults, with Austin having a lower proportion at risk for complications for COVID-19 than the national average; for 25-39 year olds the high risk proportion is slightly higher than the national average.

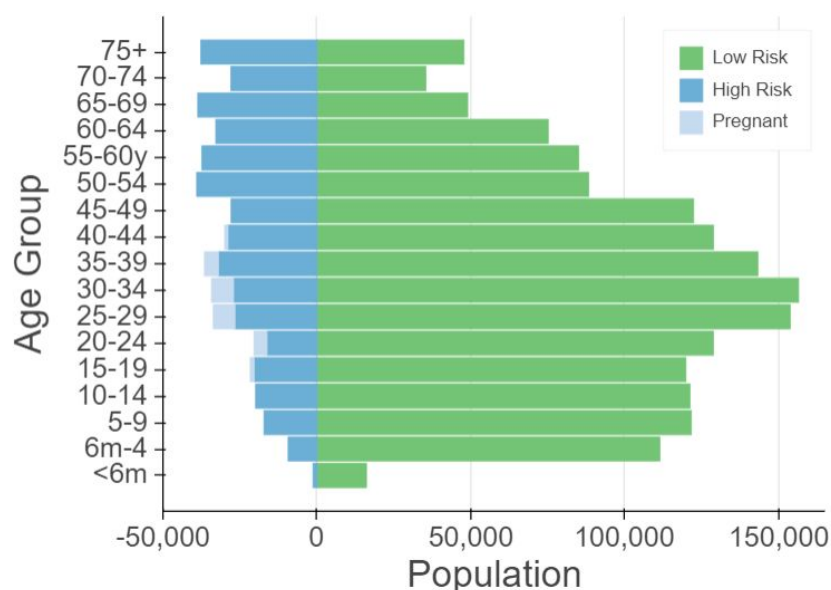


Figure A2. Demographic and risk composition of the Austin-Round Rock MSA. Bars indicate age-specific population sizes, separated by low risk, high risk, and pregnant. High risk is defined as individuals with cancer, chronic kidney disease, COPD, heart disease, stroke, asthma, diabetes, HIV/AIDS, and morbid obesity, as estimated from the CDC 500 Cities Project,[18] reported HIV prevalence[21] and reported morbid obesity prevalence,[22,23] corrected for multiple conditions. The population of pregnant women is derived using the CDC's method combining fertility, abortion and fetal loss rates.[29–31]

Table A6. High-risk conditions for influenza and data sources for prevalence estimation

Condition	Data source
Cancer (except skin)	CDC 500 cities[18]
Chronic kidney disease	CDC 500 cities[18]
COPD	CDC 500 cities[18]
Coronary heart disease	CDC 500 cities[18]
Stroke	CDC 500 cities[18]
Asthma	CDC 500 cities[18]
Diabetes	CDC 500 cities[18]
HIV/AIDS	CDC HIV Surveillance report[21]
Obesity	CDC 500 cities complemented with Sturm and Hattori[22] and Morgan et al.[23]
Pregnancy	National Vital Statistics Reports[29] and abortion data[30]

Table A7: Comparison between published national estimates and Austin-Round Rock MSA estimates of the percent of the population at high-risk of influenza/COVID-19 complications

Age Group	National estimates[27]	Austin (excluding pregnancy)	Pregnant women (proportion of age group)
0 to 6 months	NA	6.8	-
6 months to 4 years	6.8	7.4	-
5 to 9 years	11.7	11.6	-
10 to 14 years	11.7	13.0	-
15 to 19 years	11.8	13.3	1.7
20 to 24 years	12.4	10.3	5.1
25 to 34 years	15.7	13.5	7.8
35 to 39 years	15.7	17.0	5.1
40 to 44 years	15.7	17.4	1.2
45 to 49 years	15.7	17.7	-
50 to 54 years	30.6	29.6	-
55 to 60 years	30.6	29.5	-
60 to 64 years	30.6	29.3	-
65 to 69 years	47.0	42.2	-
70 to 74 years	47.0	42.2	-
75 years and older	47.0	42.2	-

References

1. Workforce overview. In: Austin Chamber of Commerce [Internet]. [cited 30 Mar 2020]. Available: <https://www.austinchamber.com/economic-development/austin-profile/workforce/overview>
2. Stay Home - Work Safe Order Information | AustinTexas.gov. [cited 30 Mar 2020]. Available: <https://austintexas.gov/article/stay-home-work-safe-order-information>
3. Li Q, Guan X, Wu P, Wang X, Zhou L, Tong Y, et al. Early Transmission Dynamics in

Wuhan, China, of Novel Coronavirus-Infected Pneumonia. *N Engl J Med*. 2020. doi:10.1056/NEJMoa2001316

4. Kraemer MUG, Yang C-H, Gutierrez B, Wu C-H, Klein B, Pigott DM, et al. The effect of human mobility and control measures on the COVID-19 epidemic in China. *medRxiv*. 2020. Available: <https://www.medrxiv.org/content/10.1101/2020.03.02.20026708v1>
5. Lauer SA, Grantz KH, Bi Q, Jones FK, Zheng Q, Meredith HR, et al. The Incubation Period of Coronavirus Disease 2019 (COVID-19) From Publicly Reported Confirmed Cases: Estimation and Application. *Ann Intern Med*. 2020. doi:10.7326/M20-0504
6. Mizumoto K, Kagaya K, Zarebski A, Chowell G. Estimating the Asymptomatic Proportion of 2019 Novel Coronavirus onboard the Princess Cruises Ship, 2020. *Infectious Diseases (except HIV/AIDS)*. *medRxiv*; 2020. doi:10.1101/2020.02.20.20025866
7. Keeling MJ, Rohani P. *Modeling Infectious Diseases in Humans and Animals*. Princeton University Press; 2011. Available: <https://play.google.com/store/books/details?id=LxzILSuKDhUC>
8. Gillespie DT. Approximate accelerated stochastic simulation of chemically reacting systems. *J Chem Phys*. 2001;115: 1716–1733. doi:10.1063/1.1378322
9. Verity R, Okell LC, Dorigatti I, Winskill P, Whittaker C, Imai N, et al. Estimates of the severity of COVID-19 disease. *Epidemiology*. *medRxiv*; 2020. doi:10.1101/2020.03.09.20033357
10. Du Z, Xu X, Wu Y, Wang L, Cowling BJ, Meyers LA. The serial interval of COVID-19 from publicly reported confirmed cases. *Epidemiology*. *medRxiv*; 2020. doi:10.1101/2020.02.19.20025452
11. CDC. People at High Risk of Flu. In: Centers for Disease Control and Prevention [Internet]. 1 Nov 2019 [cited 26 Mar 2020]. Available: <https://www.cdc.gov/flu/highrisk/index.htm>
12. CDC - BRFSS. 5 Nov 2019 [cited 26 Mar 2020]. Available: <https://www.cdc.gov/brfss/index.html>
13. Zhang X, Holt JB, Lu H, Wheaton AG, Ford ES, Greenlund KJ, et al. Multilevel regression and poststratification for small-area estimation of population health outcomes: a case study of chronic obstructive pulmonary disease prevalence using the behavioral risk factor surveillance system. *Am J Epidemiol*. 2014;179: 1025–1033. doi:10.1093/aje/kwu018
14. Calendar of Events. In: Austin ISD [Internet]. [cited 26 Mar 2020]. Available: <https://www.austinisd.org/calendar>
15. Tindale L, Coombe M, Stockdale JE, Garlock E, Lau WYV, Saraswat M, et al. Transmission interval estimates suggest pre-symptomatic spread of COVID-19. *Epidemiology*. *medRxiv*; 2020. doi:10.1101/2020.03.03.20029983
16. `minimize(method='trust-constr')` — SciPy v1.4.1 Reference Guide. [cited 28 Mar 2020]. Available: <https://docs.scipy.org/doc/scipy/reference/optimize.minimize-trustconstr.html>

17. Prem K, Cook AR, Jit M. Projecting social contact matrices in 152 countries using contact surveys and demographic data. *PLoS Comput Biol*. 2017;13: e1005697. doi:10.1371/journal.pcbi.1005697
18. 500 Cities Project: Local data for better health | Home page | CDC. 5 Dec 2019 [cited 19 Mar 2020]. Available: <https://www.cdc.gov/500cities/index.htm>
19. Health Outcomes | 500 Cities. 25 Apr 2019 [cited 28 Mar 2020]. Available: <https://www.cdc.gov/500cities/definitions/health-outcomes.htm>
20. Part One: Who Lives with Chronic Conditions. In: Pew Research Center: Internet, Science & Tech [Internet]. 26 Nov 2013 [cited 23 Nov 2019]. Available: <https://www.pewresearch.org/internet/2013/11/26/part-one-who-lives-with-chronic-conditions/>
21. for Disease Control C, Prevention, Others. HIV surveillance report. 2016; 28. URL: <http://www.cdc.gov/hiv/library/reports/hiv-surveillance.html> Published November. 2017.
22. Sturm R, Hattori A. Morbid obesity rates continue to rise rapidly in the United States. *Int J Obes*. 2013;37: 889–891. doi:10.1038/ijo.2012.159
23. Morgan OW, Bramley A, Fowlkes A, Freedman DS, Taylor TH, Gargiullo P, et al. Morbid obesity as a risk factor for hospitalization and death due to 2009 pandemic influenza A(H1N1) disease. *PLoS One*. 2010;5: e9694. doi:10.1371/journal.pone.0009694
24. Estimating the Number of Pregnant Women in a Geographic Area from CDC Division of Reproductive Health. Available: <https://www.cdc.gov/reproductivehealth/emergency/pdfs/PregnacyEstimateBrochure508.pdf>
25. Miller GF, Coffield E, Leroy Z, Wallin R. Prevalence and Costs of Five Chronic Conditions in Children. *J Sch Nurs*. 2016;32: 357–364. doi:10.1177/1059840516641190
26. Cancer Facts & Figures 2014. [cited 30 Mar 2020]. Available: <https://www.cancer.org/research/cancer-facts-statistics/all-cancer-facts-figures/cancer-facts-figures-2014.html>
27. Hales CM, Fryar CD, Carroll MD, Freedman DS, Ogden CL. Trends in Obesity and Severe Obesity Prevalence in US Youth and Adults by Sex and Age, 2007–2008 to 2015–2016. *JAMA*. 2018;319: 1723–1725. doi:10.1001/jama.2018.3060
28. Zimmerman RK, Lauderdale DS, Tan SM, Wagener DK. Prevalence of high-risk indications for influenza vaccine varies by age, race, and income. *Vaccine*. 2010;28: 6470–6477. doi:10.1016/j.vaccine.2010.07.037
29. Martin JA, Hamilton BE, Osterman MJK, Driscoll AK, Drake P. Births: Final Data for 2017. *Natl Vital Stat Rep*. 2018;67: 1–50. Available: <https://www.ncbi.nlm.nih.gov/pubmed/30707672>
30. Jatlaoui TC, Boutot ME, Mandel MG, Whiteman MK, Ti A, Petersen E, et al. Abortion Surveillance - United States, 2015. *MMWR Surveill Summ*. 2018;67: 1–45.

doi:10.15585/mmwr.ss6713a1

31. Ventura SJ, Curtin SC, Abma JC, Henshaw SK. Estimated pregnancy rates and rates of pregnancy outcomes for the United States, 1990-2008. *Natl Vital Stat Rep.* 2012;60: 1–21. Available: <https://www.ncbi.nlm.nih.gov/pubmed/22970648>